High frequency sound velocity in the glass former $2Ca(NO_3)_2 \cdot 3KNO_3$: Molecular dynamics simulations

Mauro C. C. Ribeiro*
Laboratório de Espectroscopia Molecular, Instituto de Química, Universidade de São Paulo, Caixa Postal 26077, CEP 05513-970 São Paulo, São Paulo, Brazil
(Received 19 December 2006; published 6 April 2007)

Molecular dynamics simulations of the fragile glass-forming liquid $2Ca(NO_3)_2 \cdot 3KNO_3$ (CKN) were performed from its molten state at 800 K down to its glassy state at 250 K. Time correlation functions of mass current fluctuations were calculated in order to investigate sound waves of high wave vectors, $0.18 < k < 0.67$ Å^{-1}. The high frequency (THz) sound velocity of CKN was obtained from the slope of the dispersion curve of excitation energy of acoustic modes, $\omega(k)$, as a function of temperature across the glass transition. The temperature dependence of the sound velocity of longitudinal acoustic modes is discontinuous in a range that is higher than the glass transition temperature T_g estimated from the T dependence of density and energy. This result demonstrates that the high frequency sound velocity probes the transition from liquidlike to solidlike regimes at a temperature higher than the T_g of the simulated material. The sound velocity of transverse acoustic (TA) modes presents discontinuity at the same value of the thermodynamic derived T_g. It is proposed that the distinct behavior of high frequency TA modes is due to fast reorientational motions of NO_3^- anions that are able to relieve local shear stresses.

DOI: 10.1103/PhysRevB.75.144202 PACS number(s): 61.43.Fs, 61.20.Ja

I. INTRODUCTION

A supercooled liquid undergoes glass transition when the arrest of molecular motions occurring at low temperature precludes that structural relaxation can be observed in an experiment. Usually, the glass transition temperature T_g of a material is determined from rather macroscopic probes, such as the sharp decrease of heat capacity or the more than ten orders of magnitude increase in viscosity upon going from the supercooled liquid to the amorphous solid state.[1,2] However, the system might present the response of a viscous (liquidlike) or an elastic (solidlike) material at a given T depending on the time scale, i.e., the frequency ω, probed in a particular experimental technique. Several orders of magnitude of ω can be tuned by using different spectroscopic techniques, allowing for the investigation of collective dynamics of supercooled liquids in a wide frequency range.[3,4] On cooling down the material, the transition between regimes will be observed when the inverse of the structural relaxation time, the so-called α relaxation τ_α, initially higher than the measurement frequency at high T, $\omega \ll 1/\tau_\alpha$, becomes very small at low T, $\omega \gg 1/\tau_\alpha$.

The molten salt mixture $2Ca(NO_3)_2 \cdot 3KNO_3$ (CKN) is a prototype fragile glass-forming liquid, i.e., a system whose viscosity increases in a non-Arrhenius pattern when approaching T_g.[5] Sound wave excitations in CKN have been investigated by ultrasonic experiments at MHz frequencies,[6,7] by Brillouin scattering spectroscopy at hypersonic (GHz) frequencies,[8–11] and, more recently, by inelastic x-ray scattering spectroscopy at THz frequencies.[12] Figure 1 collects the results of sound velocity of CKN as a function of temperature reported in these works. (When cooling CKN, the calorimetric glass transition is observed at $T_g = 335$ K; on heating, two melting temperatures T_m, indicating distinct crystalline structures, are observed at 425 and 444 K.[13]) The figure shows the transition of the velocity of propagation of longitudinal acoustic modes v_{LA} from the low frequency limit in the normal liquid state to the high frequency limit in the glassy state, in which the structure is frozen with respect to the frequency of the measured excitations, $\omega \gg 1/\tau_\alpha$. Figure 1 also illustrates that v_{LA} depends markedly on the actual frequency that is being probed in a particular experiment, so that, for a fixed temperature in the $T_g < T < T_m$ range, v_{LA} increases when the excitations change from MHz to GHz frequencies.

A single value at THz frequency was reported in Ref. 12 for glassy CKN at room temperature (see v_{LA} at 293 K in Fig. 1). Investigation of fast collective properties of short

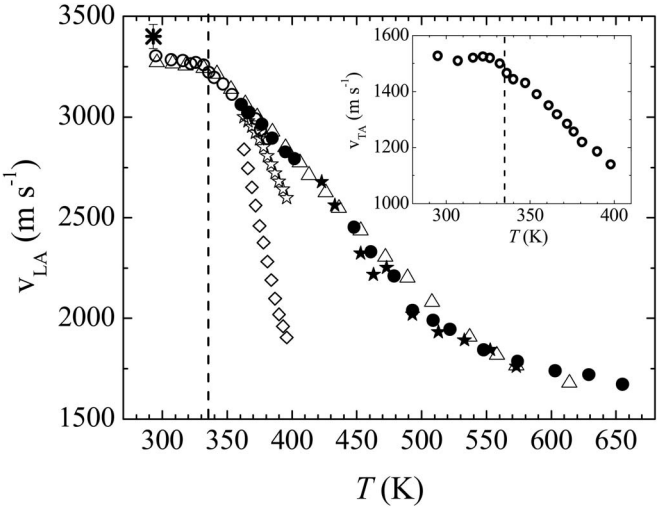

FIG. 1. The temperature dependence of sound velocity of longitudinal acoustic (LA) modes of CKN at different frequencies: (◇) 1.0 MHz, Ref. 6; (☆) 0.2 GHz, Ref. 6; (●) 10.0 GHz, Ref. 8; (○) 10.0 GHz, Ref. 9; (△) 10.0 GHz, Ref. 10; (★) 10.0 GHz, Ref. 11; (∗) 1.0 THz, Ref. 12. The inset shows the corresponding data of Ref. 9 for transverse acoustic (TA) modes. The vertical dotted line indicates the calorimetric glass transition temperature, $T_g = 335$ K (Ref. 13).

wavelength, i.e., in the high wave vector and frequency (k,ω) range, is the domain of inelastic neutron (INS) or x-ray (IXS) scattering spectroscopies.[14] The temperature dependence of excitation energies of sound modes at high (k,ω) range obtained by IXS measurements on molecular glass formers shows a discontinuity at a temperature T_x that is higher than the calorimetric T_g.[15] This finding indicates that a liquid-glass transition is occurring at THz frequency proper to an arrest of relaxations at the molecular scale, since IXS probes wave vectors larger than ~ 0.1 Å^{-1}. In other words, whereas T_g indicates the macroscopic arrest of structural relaxation, T_x indicates a microscopic liquid-glass transition. The ratio T_x/T_g depends on the studied glass former; for instance, in the case of *o*-terphenyl, T_x is very close to T_g.[15,16] This finding was corroborated by molecular dynamics (MD) simulations,[17] in which the dynamic structure factor $S(k,\omega)$ of *o*-terphenyl was calculated as a function of temperature.

The THz range is the typical range accessible by computer simulations of liquids. Due to limitations in computational resources, computer prepared glasses undergo quenching rates that are approximately ten orders of magnitude higher than common laboratory conditions. As a consequence of such high quenching rates, a "smearing out" of the liquid-solid transition occurs, i.e., the glass transition region because less sharp at very high quenching rates than at the usual quenching condition. As discussed by Angell and Torell,[18] the wide temperature range in which the response of the system changes from liquidlike to solidlike should be called the "dispersion region" in fast quenching experiments. Interestingly, the smearing out of the glass transition can also be observed in real samples prepared at low quenching rates provided that enough high frequency relaxations could be probed in the experiment. This proposition was illustrated by Angell and Torell[18] with the Brillouin light scattering results of CKN at GHz frequency reported by Torell (black circles in Fig. 1),[8] where a change in slope of the $v_{\mathrm{LA}}(T)$ plot is observed at 500 K, which is much higher than the calorimetric T_g. However, the results reported by Torell[8] covered only the $361<T<655$ K range, i.e., above the calorimetric T_g. When Brillouin measurements on CKN were further extended to low T,[9,10] they revealed a sharp discontinuity of $v_{\mathrm{LA}}(T)$ at the calorimetric T_g (white triangles and white circles in Fig. 1). The results of Torell and Aronsson[9] for the sound velocity of transverse acoustic excitations v_{TA}, shown in the inset of Fig. 1, also show a sharp transition from liquidlike to solidlike values at T_g.

As pointed out above, we do not have a complete picture of sound velocity in CKN at THz frequency. The aim of this work is to investigate the temperature dependence of acoustic excitations at THz range in CKN by MD simulation. In a previous MD investigation of CKN,[19] the nature of acoustic and optic modes of CKN has been studied in a wide wave-vector range, $0.2<k<7.0$ Å^{-1}. At the time that this MD study was reported, the x-ray result of Ref. 12 for glassy CKN was published. In Ref. 12, the sound velocity of CKN at THz frequency was obtained from the dispersion curve of excitation energy, $\omega(k)$, obtained in the $0.13<k<0.8$ Å^{-1} range. In this work, MD simulations were performed with a larger number of particles than in the previous study,[19] so that more data for k below 0.8 Å^{-1} could be recorded, enabling the calculation of the sound velocity. Contrary to the previous study,[19] in which the simulations were performed at fixed temperature, LA and TA modes of CKN are investigated here as a function of temperature across the glass transition of the simulated system. The temperature dependence of calculated single-particle properties such as diffusion coefficient, reorientational relaxation, and the self-part of the intermediate scattering function has already been reported.[20] Thus, the aim of this work is to show that high frequency collective dynamics might point to a liquid-solid transition at T_x that is higher than T_g, the latter determined as usual from discontinuity on the temperature dependence of density, energy, or diffusion coefficient, given the *same* (high) quenching rate experienced by the material.

II. COMPUTATIONAL DETAILS

The MD simulations were performed with a polarizable model that was originally proposed for the study of the equilibrium structure and basic dynamical properties of CKN in its molten state.[21,22] The potential-energy function contains a pairwise additive part, given by a Born-Mayer potential as it is usual for simulation of molten salts, plus a fluctuating charge (FC) model that accounts for polarization effects on the NO_3^- anions. In the FC model, the partial charges assigned to the atoms of a given NO_3^- anion are not fixed; instead, they fluctuate during the simulation due to the changing environment experienced by the ion.[23] Charge transfer is not allowed between different anions, and the K^+ and the Ca^{2+} species carry their full formal charge (no polarization effects are considered for cations). The magnitude of charge transfer between atoms inside a given anion is dictated by the difference in the instantaneous electronegativity of each atom. At each time step of the MD run, atomic electronegativities are calculated by a quadratic expansion of the electrostatic energy. Thus, partial charges of NO_3^- species are updated simultaneously with ionic coordinates, in a similar fashion as Carr-Parrinello MD simulations. The parameters in the expansion of the electrostatic energy that determine the charge fluctuation in the NO_3^- species were corroborated by *ab initio* calculations.[24] More details about the implementation of the polarizable model in the MD simulation, and parameters of the FC model for CKN, can be found in Refs. 21 and 24.

In the previous investigation of collective dynamics of CKN at a single temperature,[19] a system made of 501 ions was considered. This system size limited the number of low-k data, precluding that reliable sound velocity could be obtained. In this work, a larger system size (996 ions) has been considered (166 Ca^{2+}, 249 K^+, and 581 NO_3^-). This system was used in the previous study of single-particle dynamics of CKN across the glass transition.[20] In Ref. 19, the long-range electrostatic interactions were handled with the Ewald sum method, whereas in Ref. 20 the Wolf method was used[25] in order to reduce computational time. The Wolf method considers a truncated shifted Coulomb potential, so that the interaction between two charges is evaluated as long as their

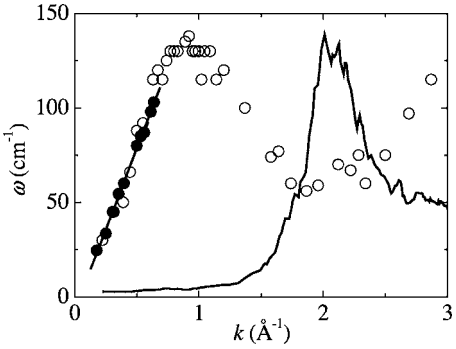

FIG. 2. Dispersion curve for LA modes of CKN at 800 K with different system sizes and protocols for handling the long-range electrostatic interactions: (○) 501 ions, and the Ewald sum method (results of Ref. 19); (●) 996 ions, and the Wolf method (Ref. 25) (this work). The full line on the black circles is a linear fit to the results of this work. In an arbitrary intensity scale, the static structure factor $S(k)$ of the simulated system is also shown as a full line.

distance is smaller than a cutoff radius. This method is equivalent to ensuring charge neutrality in the spherical volume around a given charge.[25] It has been shown that both the Ewald sum and the Wolf method give the same ionic mean-square displacement and the same decay rate of reorientational time correlation function and intermediate scattering function of CKN (see Fig. (1) in Ref. 20). Recently, good agreement has been found for several thermodynamics, equilibrium, and dynamics properties of molecular and ionic systems simulated with the Wolf method and the Ewald sum method.[26] In this work, it is mandatory to compare whether excitation energies of acoustic modes calculated with the Wolf method agree with previous results obtained with the Ewald sum method.[19] Figure 2 compares the dispersion curve of LA modes of CKN at 800 K calculated with the Ewald sum method and a system size of 501 ions (as in Ref. 19) with the results of this work calculated with the Wolf method and a system size of 996 ions. The agreement between the two protocols of simulation is clear. It is also evident that the larger system gives a nice linear relationship between ω and k in the range $0.18<k<0.64$ Å^{-1}, from which the high frequency sound velocity is determined. (The smallest accessible wave vector, $\mathbf{k}=2\pi L^{-1}[1,0,0]$, is given by the typical length of the simulation box, $L\sim 34.0$ Å.)

The same protocol used in Ref. 20 was considered for cooling down the system: from a well-equilibrated configuration at 800 K, the temperature was decreased at 50 K steps to the smallest temperature of 250 K. Equilibration period at each temperature was typically 1.0 ns, plus 1.0 ns for data acquisition (the time step was 1.0 fs). Temperature and pressure were controlled by the method of weak coupling to a bath as proposed by Berendsen *et al.*[27] The NO_3^- anion was considered as a rigid body, and a quaternion method was used to solve the rotational equations of motion.[28] Spectra of LA and TA modes were obtained by Fourier transforming the corresponding time correlation functions of mass current fluctuations.[19,29,30] Examples of calculated LA and TA spectra of CKN at fixed temperature can be found in the previous publication.[19] The excitation energy at a given wave vector is obtained from the frequency of the maximum of the current

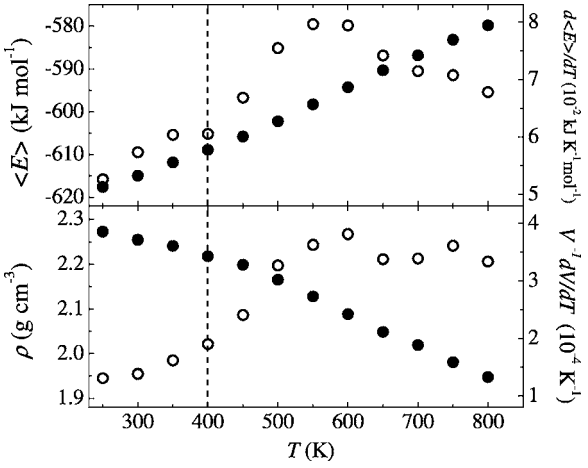

FIG. 3. Temperature dependence of configurational energy (top panel) and density (bottom panel) of CKN simulated with the polarizable FC model (black circles with scale on the left). The white circles are the corresponding numerical derivatives (scale on the right). The vertical dashed line at 400 K marks the "calorimetric" T_g of simulated CKN that will be used in the following comparisons.

spectra, and the slope of $\omega(k)$ plots provides the apparent sound velocity at THz range for each temperature. Further computational details can be found in previous publications.[19–22]

III. RESULTS AND DISCUSSION

The temperature dependence of average density ρ and configurational energy E of simulated CKN are shown in Fig. 3 by black circles. The dispersion region in which ρ and E change from liquidlike to solidlike values is better appreciated by the corresponding derivatives (white circles in Fig. 1) that are related to the thermal-expansion coefficient and heat capacity. The pattern of these derivatives resembles experimental data recorded with typical laboratory cooling rates, but with a dispersion region that extends for a much broader temperature range. In the case of simulated CKN, the dispersion region covers ~200°, whereas the transition in laboratory prepared glassy CKN takes place in ~20°. Identification of T_g in MD simulations is usually accomplished from the change in slope of $\rho(T)$ and $E(T)$ curves, although the temperature behavior of diffusion coefficient D is also used.[31,32] In the previous investigation of single-particle dynamics of CKN,[20] it has been identified that $T_g=380\pm 20$ K from density and dynamical properties of the simulated system. Although significant enhancement of ionic mobility in CKN is observed when including polarization effects in the simulations,[20,22] the resulting T_g of the simulated system with the FC model is still higher than the experimental T_g. The mismatch between simulated and experimental T_g is not necessarily due to a drawback of the model; it should be assigned instead to the very fast cooling rate in the MD simulations. Nevertheless, the focus here is to compare the "calorimetric" T_g of the simulated system with the liquid-solid transition as probed by the high frequency sound ve-

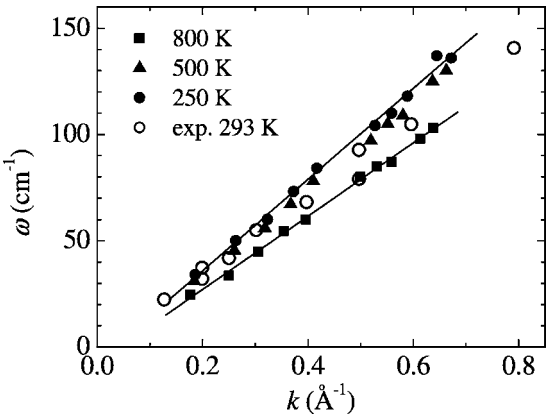

FIG. 4. Dispersion curves of longitudinal acoustic (LA) modes of simulated CKN at indicated temperatures (black symbols). The full lines are linear fits to the 250 and 800 K results. The white circles are experimental data available for glassy CKN at 293 K (Ref. 12).

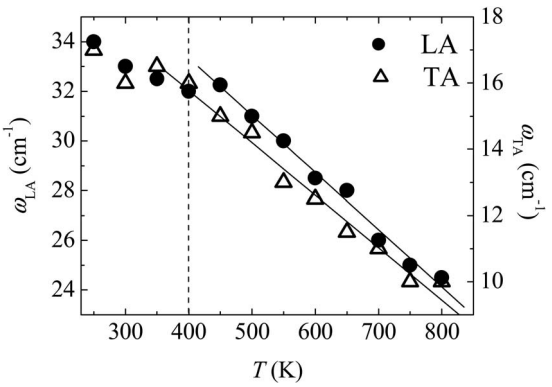

FIG. 5. Temperature dependence of the excitation energy of LA and TA modes of CKN, respectively, black circles and white triangles, at the smallest wave vector accessible in the MD simulations, $\mathbf{k}=2\pi L^{-1}[1,0,0]$. The scale for TA excitation energy is on the right. As a guide for the eyes, the full lines show linear fits to the high-temperature range. The vertical dashed line at 400 K is T_g of the simulated system as estimated in Fig. 3.

locity. In Ref. 18, approximate temperature scaling of compressibility data of CKN was performed in order to compare the glass transition of CKN with simulation results for a simple Lennard-Jones model system with parameters characteristic of argon. In this work, T_g, as estimated from Fig. 3 shall be compared with the transition region revealed by the high frequency collective dynamics for the same system undergoing the same quenching rate. Thus, the vertical dashed line drawn at 400 K in Fig. 3 marks the change of slope of $\rho(T)$ and $E(T)$ curves, as it is usually associated with T_g in MD simulations, which will be used in the following analysis instead of the experimental T_g of real CKN.

Since simulated T_g seems higher than the real system T_g, it is mandatory to first verify whether calculated excitation energies of high frequency LA modes of CKN are reasonable in comparison with experimental data. Such a comparison was not possible at the time that the collective dynamics of 501 ions simulated at fixed T was reported,[19] since the x-ray results of Matic *et al.*[12] was published simultaneously with Ref. 19. Dispersion curves of LA modes calculated in this work with the 996-ion system are shown in Fig. 4 for some temperatures together with the single temperature data reported in Ref. 12 for glassy CKN. A nice linear $\omega(k)$ relationship is observed within the $0.2<k<0.7$ Å^{-1} range, whose slope is comparable with experimental data. Since the potential-energy function was not built specifically for studying the acoustic modes, the agreement with experiment should be considered satisfactory, indicating that the stiffness of the polarizable FC model for CKN is realistic.

Figure 5 shows excitation energies of LA and TA modes as a function of temperature for a fixed k, namely, the smallest wave vector accessible in the MD simulations. The wave number of LA excitations seems to saturate at a temperature T_x that is close to the calorimetric T_g previously determined in Fig. 3. One can say that T_x estimated from the excitation energy of the high frequency LA modes is ~10% higher than T_g, since T_g itself is not a sharp value. More interesting, however, is the finding that the energy excitation of TA modes is discontinuous at a T_x that is lower than the T_x value indicated by the LA modes. In other words, Fig. 5 suggests that $\omega(T)$ at fixed k bends within a T range that is lower for TA modes than for LA modes. Plots similar to Fig. 5 have been obtained by inelastic x-ray scattering measurements of LA modes of *n*-butyl-benzene, *o*-terphenyl, and glycerol.[15] Observed ratio T_x/T_g ranged from ≈1 for *n*-butyl-benzene to ≈1.6 for glycerol, indicating a correlation between T_x/T_g and fragility. Excitation energies in Fig. 5 correspond to a single k, but the actual T_x depends on k, as already observed by MD simulations of *o*-terphenyl,[17] where the difference between T_x and T_g increased for LA modes of higher k. Unfortunately, corresponding results for TA modes of *o*-terphenyl were not reported in Ref. 17. Thus, the most important conclusion that can be drawn from Fig. 5 is that the comparison between LA and TA modes of CKN strongly suggests that, as far as TA excitations are concerned, the structure at the molecular scale is not yet frozen at the same T_x as LA excitations suggest.

The high frequency sound velocity of CKN was obtained from linear fits to dispersion curves $\omega(k)$ for each temperature. The resulting temperature dependence of sound velocity of LA and TA modes, v_{LA} and v_{TA}, is shown in Fig. 6. It is clear from Fig. 6 that T_x for LA modes is higher than the corresponding value for TA modes. The $v_{\mathrm{LA}}(T)$ curve gives a T_x that is ~25% larger than T_g, whereas the $v_{\mathrm{TA}}(T)$ curve is discontinuous at essentially the same calorimetric T_g. Thus, Fig. 6 demonstrates the assertion that a high frequency probe such as high-(k,ω) LA modes will reveal a liquid-solid transition at a higher temperature than thermodynamics properties, given the same (high) cooling rate experienced by the material. On the other hand, Fig. 6 adds another piece of information, as TA modes continue to experience some local structural relaxation down to T_g.

In the previous investigation of the single-particle dynamics of CKN,[20] diffusion coefficient D, reorientational relaxation time τ_{or}, and structural relaxation time τ_α of the self-part of the intermediate scattering function $F_s(\mathbf{k},t)$ of NO_3^- anions were calculated. Whereas $F_s(\mathbf{k},t)$ reached a plateau at

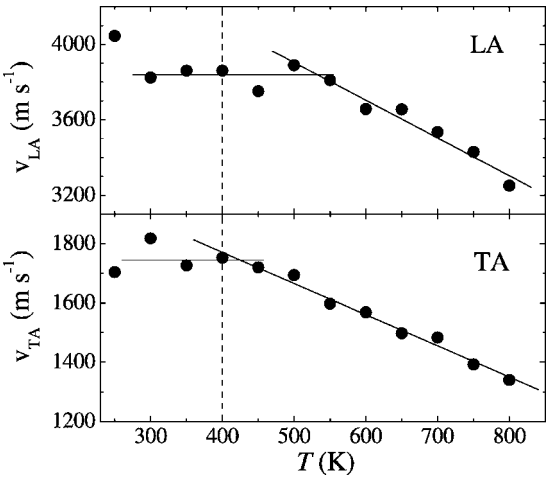

FIG. 6. The temperature dependence of the high frequency sound velocity of LA modes (top panel) and TA modes (bottom panel) of CKN. As a guide for the eyes, the full lines show linear fits to either low- or high-temperature ranges. The vertical dashed line at 400 K is T_g of the simulated system as estimated in Fig. 3.

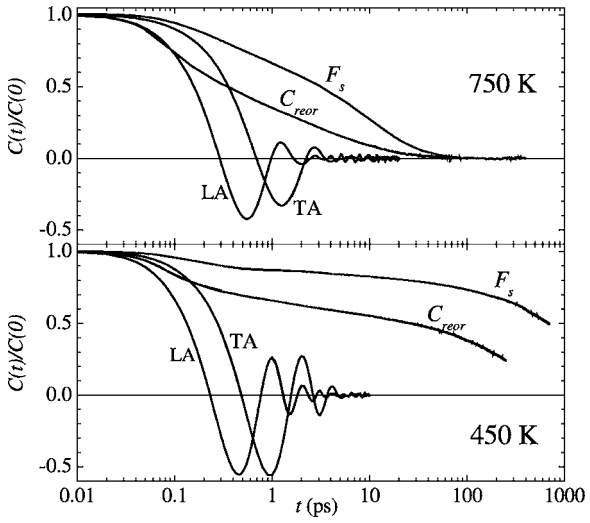

FIG. 7. A comparative perspective of several time correlation functions of CKN at 750 and 450 K. The figure shows the self-part of the intermediate scattering function $F_s(\mathbf{k},t)$ at $k=1.46$ Å and the reorientational time correlation function $C_{reor}(t)$ of NO_3^- anions as previously reported in Ref. 20. These are compared with the time correlation functions of longitudinal and transverse mass current fluctuations calculated in this work for the smallest accessible wave vector.

T_g, indicating that τ_α diverged and local-density fluctuations became frozen at T_g, the reorientational time correlation function $C_{reor}(t)$ still decayed at T below T_g so that it was possible to measure τ_{or} at low T. When D, τ_{or}, and τ_α are plotted together as a function of temperature, all of them display the same activation energy in the high-T range, and then they decouple for T below ~500 K (see Fig. 6 of Ref. 20). Thus, decoupling between these different dynamical processes occurs in the same temperature range in which v_{LA} saturate to the solidlike value (see Fig. 6). Furthermore, it is worth noting that $T\sim 500$ K is also the range in which experimental $v_{\mathrm{LA}}(T)$ curves at GHz frequency present the first change in slope (see Fig. 1). This first discontinuity observed in $v_{\mathrm{LA}}(T)$ at GHz well above T_g might also be due to the same dynamical decoupling observed in the MD simulations, which is much more evident when the probe is v_{LA} at THz frequency.

In Ref. 20, the self-part of van Hove correlation function $G_s(r,t)$ of NO_3^- anions and its reorientational counterpart, $G_{or}(\theta,t)$, related to the evolution of the angle $\theta(t)$ made by a unitary vector along the C_3 axis of a given NO_3^- anion at distinct times, were calculated. At low temperature (400 K), where $G_s(r,t)$ indicates that diffusion is essentially frozen, $G_{or}(\theta,t)$ clearly indicates that rotational hopping processes are still taking place (see Fig. 9 of Ref. 20). Rapid reorientational dynamics that decouples from translational dynamics, and that persists at low temperature, has been revealed by Raman,[33] NMR,[34] and transient optical Kerr effect[35] measurements of CKN. In the case of quinoline,[36] neutron-scattering spectroscopy revealed coupling between shear and reorientational dynamics, and indicated that fast librational motions would be able to relieve local stresses. It is proposed here that large angle jumps occurring in the simulated CKN at low T are the origin of the distinct behavior of $v_{\mathrm{TA}}(T)$ and $v_{\mathrm{LA}}(T)$ curves in Fig. 6. Since these different dynamical processes span an extended time range, it would be useful to have a perspective view of the relevant time correlation functions in order to verify whether this proposition is a reasonable one. Figure 7 provides in a single plot a comparison of $F_s(\mathbf{k},t)$, $C_{reor}(t)$, $C_{\mathrm{LA}}(t)$, and $C_{\mathrm{TA}}(t)$ of CKN simulated at 750 (top panel) and 450 K (bottom panel). It is clear that translational, reorientational, and collective dynamics are all coupled together at high T. At low T, the time correlation functions of mass current fluctuations display an oscillatory pattern in a much shorter time range than the overall dynamics of diffusive and reorientational motions. However, it is interesting to note that the initial fast decay of $C_{reor}(t)$ at 450 K still overlaps the initial decay of $C_{\mathrm{TA}}(t)$, in which the latter decays to ~0.8 of its zero time value. Thus, the assumption of Ref. 36 for liquid quinoline, i.e., it uses fast librations as an efficient mechanism to relieve microscopic stresses, seems also a reasonable one for CKN. In summary, the density fluctuations of high k that are probed by the LA modes are frozen at T_x higher than T_g, so that v_{LA} reaches solidlike values at $T\sim 500$ K, but v_{TA} continues to increase with further decrease of T because local relaxations still remain down to T_g of simulated CKN.

IV. CONCLUSIONS

The archetypical fragile ionic glass-former CKN has been simulated with the polarizable FC model in a wide temperature range covering the well-equilibrated liquid state down to the deeply cooled glassy state. The main upshot of the MD simulations was to demonstrate that the high frequency sound velocity of LA modes probes the liquid-solid transition in a temperature that is higher than the T_g estimated from thermodynamic properties of the same material undergoing the same quenching rate. The temperature in which

v_{LA} reaches its solidlike value is the same as that in which decoupling between D, τ_{or}, and τ_{α} was previously observed.[20] Conversely, the temperature discontinuity of the sound velocity of TA modes occurs at the calorimetric T_g of the simulated system. In Ref. 20, it was demonstrated that fast reorientational dynamics due to angular hopping processes continues to be active at low temperature. It is proposed here that this microscopic dynamics would be able to relieve local stresses in CKN at low T, when the structural arrest has already taken place and density fluctuations are almost frozen. It is our hope that further IXS measurements of the high frequency sound velocity of CKN could reveal the distinct temperature dependence between LA and TA modes as anticipated by these MD simulations.

ACKNOWLEDGMENTS

The author is indebted to FAPESP and CNPq for financial support.

*Electronic address: mccribei@iq.usp.br

[1] S. R. Elliot, *Physics of Amorphous Materials* (Longman, Harlow, 1990).
[2] A. K. Varshneya, *Fundamentals of Inorganic Glasses* (Academic, New York, 1994).
[3] K. L. Ngai, J. Non-Cryst. Solids **275**, 7 (2000).
[4] P. Lukenheimer, U. Schneider, R. Brand, and A. Loidl, Contemp. Phys. **41**, 15 (2000).
[5] C. A. Angell, P. H. Poole, and J. Shao, Nuovo Cimento D **16**, 993 (1994).
[6] R. Weiler, R. Bose, and P. B. Macedo, J. Chem. Phys. **53**, 1258 (1970).
[7] L.-T. Cheng, Y.-X. Yan, and K. A. Nelson, J. Chem. Phys. **91**, 6052 (1989).
[8] L. M. Torell, J. Chem. Phys. **76**, 3467 (1982).
[9] L. M. Torell and R. Aronsson, J. Chem. Phys. **78**, 1121 (1983).
[10] G. Li, W. M. Du, J. Hernandez, and H. Z. Cummins, Phys. Rev. E **48**, 1192 (1993).
[11] E. A. Pavlatou, A. K. Rizos, G. N. Papatheodorou, and G. Fytas, J. Chem. Phys. **94**, 224 (1991).
[12] A. Matic, L. Börjesson, G. Ruocco, C. Masciovecchio, A. Mermet, F. Sette, and R. Verbeni, Europhys. Lett. **54**, 77 (2001).
[13] E. Kartini, M. F. Collins, B. Collier, F. Mezei, and E. C. Svensson, Can. J. Phys. **73**, 748 (1995).
[14] G. Ruocco and F. Sette, J. Phys.: Condens. Matter **11**, R259 (1999).
[15] C. Masciovecchio, G. Monaco, G. Ruocco, F. Sette, A. Cunsolo, M. Krisch, A. Mermet, M. Soltwisch, and R. Verbeni, Phys. Rev. Lett. **80**, 544 (1998).
[16] G. Monaco, C. Masciovecchio, G. Ruocco, and F. Sette, Phys. Rev. Lett. **80**, 2161 (1998).
[17] S. Mossa, G. Monaco, G. Ruocco, M. Sampoli, and F. Sette, J. Chem. Phys. **116**, 1077 (2002).
[18] C. A. Angell and L. M. Torell, J. Chem. Phys. **78**, 937 (1983).
[19] M. C. C. Ribeiro, J. Chem. Phys. **114**, 6714 (2001).
[20] M. C. C. Ribeiro, J. Phys. Chem. B **107**, 9520 (2003).
[21] M. C. C. Ribeiro, Phys. Rev. B **61**, 3297 (2000).
[22] M. C. C. Ribeiro, Phys. Rev. B **63**, 094205 (2001).
[23] A. W. Rick, S. J. Stuart, and B. J. Berne, J. Chem. Phys. **101**, 6141 (1994).
[24] M. C. Ribeiro and L. C. J. Almeida, J. Chem. Phys. **113**, 4722 (2000).
[25] D. Wolf, P. Keblinski, S. R. Phillpot, and J. Eggebrecht, J. Chem. Phys. **110**, 8254 (1999).
[26] C. J. Fennell and J. D. Gezelter, J. Chem. Phys. **124**, 234104 (2006).
[27] H. J. C. Berendsen, J. P. M. Postma, W. F. Gunsteren, A. DiNola, and J. R. Haak, J. Chem. Phys. **81**, 3684 (1984).
[28] M. P. Allen and D. Tildesley, *Computer Simulation of Liquids* (Clarendon, Oxford, 1987).
[29] J. P. Hansen and I. R. McDonald, *Theory of Simple Liquids* (Academic, London, 1990).
[30] U. Balucani and M. Zoppi, *Dynamics of the Liquid State* (Oxford University Press, Oxford, 1994).
[31] J.-L. Barrat and M. L. Klein, Annu. Rev. Phys. Chem. **42**, 23 (1991).
[32] W. Kob, J. Phys.: Condens. Matter **11**, R85 (1999).
[33] P. Jacobsson, L. Börjesson, A. K. Hassan, and L. M. Torell, J. Non-Cryst. Solids **172-174**, 161 (1994).
[34] S. Sen and J. F. Stebbins, Phys. Rev. B **58**, 8379 (1998).
[35] M. Ricci, P. Foggi, R. Righini, and R. Torre, J. Chem. Phys. **98**, 4892 (1993).
[36] F. J. Bermejo, M. García-Hernández, W. S. Howells, R. Burriel, F. J. Mompeán, and D. Martin, Phys. Rev. E **48**, 2766 (1993).